TẠP CHÍ KHOA HỌC
TRƯỜNG ĐẠI HỌC QUY NHƠN

Độ bền ăn mòn và bền mài mòn của các lớp phủ điện hóa Nano-, Micro chức năng

Nguyễn Đức Hùng[1*], Lê Thị Phương Thảo[2], Mai Văn Phước[3], Trần Thị Vân Nga[4]

[1]Viện Công nghệ môi trường, VAST, 18 Hoàng Quốc Việt, Quận Cầu Giấy, Hà Nội
[2]Trường Đại học Mỏ - Địa chất, 18 Phố Viên, Quận Bắc Từ Liêm, Hà Nội
[3]Viện Hóa học - Vật liệu, 17 Hoàng Sâm, Quận Cầu Giấy, Hà Nội
[4]Trường Đại học Giao thông vận tải, Cầu Giấy, Quận Đống Đa, Hà Nội

Ngày nhận bài: 23/11/2018; Ngày nhận đăng: 07/01/2019

TÓM TẮT

Các lớp phủ điện hóa chức năng: Ni-TiO_2 kỵ nước, Ni-CeO_2-CuO xúc tác, và Ni-CBN cắt, mài mòn đều cần phải bền và chống ăn mòn để đảm bảo sự ổn định trong quá trình sử dụng. Sự hiện diện của các hạt nano và micro trơ về mặt hóa học trong lớp phủ tổ hợp dẫn đến thay đổi kết cấu bề mặt và tăng khả năng chống ăn mòn. Các hạt nano TiO_2 có tính kỵ nước cao, làm giảm sự ngưng tụ độ ẩm bề mặt và giảm tốc độ ăn mòn xuống i_{Corr} = 2,23.10^{-7} A/dm^2 (1,14.10^{-4} mm/năm). Các hạt nano CeO_2-CuO trơ về mặt hóa học, do đó sự hiện diện của chúng trong các lớp nanocomposite Ni-CeO_2 cũng làm thay đổi cấu trúc bề mặt, tính chất điện hóa và cơ học của vật liệu composite. Do đó, tốc độ ăn mòn cũng giảm xuống $i_{Corr.}$ = 1,601.10^{-5} A/dm^2 (0,1972 mm/năm). Tương tự, sự hiện diện của các hạt CBN cứng và trơ về mặt hóa học trong lớp phủ tổ hợp micro Ni-CBN cũng làm tăng khả năng bền mài mòn đối với giá trị G là 1789,06 tương đương với sản phẩm của Nhật Bản và giảm tốc độ ăn mòn với $i_{Corr.}$ = 7,713. 10^{-6} A/dm^2 (4,253.10^{-2} mm/năm).

Từ khóa: *Lớp mạ điện hóa nano, micro chức năng, bền ăn mòn, lớp mạ xúc tác, lớp mạ kỵ nước, lớp mạ mài cắt.*

[*]Tác giả liên hệ chính.
Email: nguyenduchung1946@gmail.com

JOURNAL OF SCIENCE
QUY NHON UNIVERSITY

Corrosionstability and abrasionstability of Nano-, Micro- functional electrochemical coatings

Nguyen Duc Hung[1*], Le Thi Phuong Thao[2], Mai Van Phuoc[3], Tran Thi Van Nga[4]

[1]Institute of Environmental Technology, VAST, 18 Hoang Quoc Viet, Cau Giay Dist., Hanoi
[2]University of Mining and Geology, 18 Pho Vien, Bac Tu Liem Dist., Hanoi
[3]Institute for Chemistry and Materials, 17 Hoang Sam St., Cau Giay Dist., Hanoi
[4]University of Transport and Communication, Cau Giay, Dong Da Dist., Hanoi

Received: 23/11/2018; Accepted: 07/01/2019

ABSTRACT

Functional electrochemical coatings: hydrophobic Ni-TiO_2, catalytic Ni-CeO_2-CuO, and cutting, abrasive Ni-CBN all need to be durable and corrosion resistant to ensure stability in usage process. The presence of chemically inert nano and micron particles in the composite coatings leads to surface texture change and corrosion resistance increase. TiO_2 nanoparticles are highly hydrophobic, reducing surface moisture condensation and corrosion speed to $i_{Corr} = 2.23.10^{-7}$A/dm^2 ($1.14.10^{-4}$ mm/year). CeO_2-CuO nanoparticles are chemically inert, so their presence in Ni-CeO_2-CuO nanocomposite layers also changes the surface structure, electrochemical and mechanical properties of the matrix. Thus, the corrosion speed also decreases to $i_{Corr.} = 1.601.10^{-5}$A/dm^2 (0.1972 mm/year). Similarly, the presence of hard and chemically inert grinding CBN particles in the micro composite coating Ni-CBN also increases the abrasion resistance to the G value of 1789.06, which is equivalent to the Japanese product, and reduces the corrosion speed to $i_{Corr.} = 7.713.10^{-6}$ A/dm^2 ($4.253.10^{-2}$ mm/year).

Keywords: *Functional electrochemical coating, corrosion resistance, catalyst plating, hydrophobic plating, grinding plating.*

1. INTRODUCTION

Functional materials all must meet required durability of corrosion and abrasion for applying in different environments. Functional plating layers are made of inert nanoparticles or microparticles[1,2], so that the nature of these particles also contributes to the increasing of corrosion resistance of the nano and micro-composite coatings of the coated metals[3,4]. Due to the compatibility with the steel material as well as the technological advantage and economic efficiency, nickel-plated solutionsare most commonly used to create functional coatings[5,6]: catalytic platings for oxidation of engine exhaust gases such as CO, C_3H_6; superhydrophobic coatings for self-cleaning surfaces as well as durable abrasives platings for cutting and grinding tools. The nanoparticles CeO_2,[7-9] CuO,[10] TiO_2 [11,12] or micropaticles CBN[13-16] used for the mentioned functional coatings are non-conductive, chemically inert, but their presence in Ni coatings has an effect on varying the corrosion speedof nickel plating[17-19]. This depends on many factors such as the structure and composition of the nano, micro composite. Since the parameters of plating technology, such as the

*Corresponding author.
Email:nguyenduchung1946@gmail.com

concentration of substances in the electrolyte solution, the diffusion process, plating time, the temperature of the electrolyte solution greatly affect the structure and composition of the coating, this will affect the corrosion resistance of Ni-composite material. The article will present the effect of the important electroplating technical parameters on the corrosion resistance of the surface of functional layers: catalytic, super hydrophobic and cutting, grinding.

2. EXPERIMENTAL

2.1. Chemicals and materials

The chemicals used to prepare the solution are $NiSO_4.7H_2O$, $NiCl_2.6H_2O$, H_3BO_3, laurylsulphate, which are analytical pure form of China. The material CeO_2, from Richest Goup Ltd. Shanghai; CuO of Shanghai's Nano Global are 40 nm in size and CBN in 96 μm from Changsha 3 better Ultra-Hard Materials Co., Ltd, China. The TiO_2 particles were synthesed by Science University of Natural Science, Hanoi National University with a particle size of 8 - 10 nm and crystalline structure was anatase.

2.2. Plating method

Nickel-plated solutions with nanoparticles of CeO_2 and CuO for the catalytic function were prepared with $NiSO_4.7H_2O$ (200 ÷ 350) g/L, H_3BO_3 30 g/L, laurylsulphate 0.1 g/L, the total content of CeO_2 + CuO is (2 ÷ 14) g/L with pH of the solution was 4 ÷ 6. Nickel-plated solution for TiO_2 nanoparticles for hydrophobic function was mixed with $NiCl_2.6H_2O$ 300 g/L, H_3BO_3 30 g/L, laurylsunphate 0.1 g/L, TiO_2 6 g/L and pH of solution 4. The electroplating solution with CBN for cutting, abrasivefunctionwas Watts solution with $NiSO_4.7H_2O$ 300 g/L, H_3BO_3 30 g/L, laurylsulphate 0.1 g/L, CBN 160 g/L and pH of 6.

Since the CeO_2, CuO, and TiO_2 particles in nanoscale, they are well distributed in the solution when the solution is stirred. Thus, it is possible to use a bath with cathode arranged vertically as normal. In order to perform the plating process, either the direct current (DC) or the pulse current, which can be controlledthe current density and duration according to the research requirements (Figure 1),[20-22] was used.

The CBN particles with size up to 100 μm are difficult to distribute in plating solution, but it is easy to agglomerate. Thus, to codeposite the CBN particles on the nickel plating layer, horizontal cathode with a reasonable rotation speed must be used (Figure 2).[23] With the arrange of cathode as shown in Figure 2, the CBN particles, when stirred at the appropriate speed, will be dispersed in solution over the cathode so that when deposited it will stick to the horizontal surface of the cathode to incorporate with Ni layer. The proper rotation speed of the electrode will ensure the uniformbonding of the CBN particles on the cathode surface.

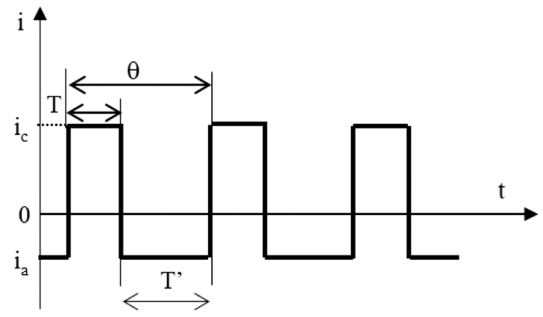

Figure 1. Reverse pulse diagram and pulse parameters: T: pulse width (pulse duration); T': Distance between two pulses (break time); θ: length of cycle; i_c: cathode current density

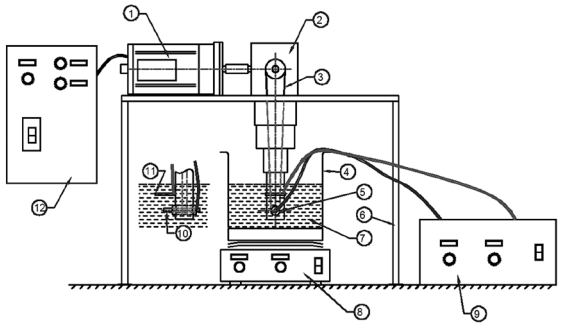

Figure 2. 1. Engine. 2. speed gearbox, 3. drive belt, 4. plating tank; 5. spinning cathode; 6. Motor support; 7. plating solution; 8. stirring machine, 9. plating source; 10. cathode; 11. anode nickel; 12. cathoderotary control box.

2.3 Evaluate the composition, structure and stability of corrosion and abrasion

The content of CuO and CeO_2, TiO_2, CBN particleson the plating layers was determined by the EDX energy scattering spectra on JMS 6610LV-JED2300, JEOL, Japan at the Institute for Chemistry and Materials/ Institute of Military Science and Technology. The surface morphology ofthe coatings was also determined through scanning electron microscope (SEM) imageswith magnifications of 1,000; 5,000 and 10,000.

The polarization curve is a graph showing the relationship between the electrode potential (E) and the response current density (i), used for studying the discharge at cathode (i_K) or the corrosion process by determining the value $i_o = i_{Corr.}$ The cathode polarization curves for Ni plating were measured in plating solution on Autolab PG302 at the Institute for Chemistry and Materials, Institute for Military Science and Technology. The working electrode was 1 cm² nickel-plated steel; the opposite electrode was Ni; reference electrode was Ag/AgCl; sweep: from open circuit (OCP) to -2.0 V; room temperature.

The impedance of Ni plating process was measured on the IM6 (Zahner - Elektrik, Germany) at the Institute of Chemistry, Academy of Science and Technology of Vietnam. When a small oscillation of voltage or current are applied on the electrochemical system, a responsive signal that issinusoida and phase-deviatory to the applied oscillation will be obtained. Measurement of the phase difference and the impedance of the electrochemical system allows analysis of electrode processessuch as diffusion, discharge kinetic, double layer or explanation of surface development of the electrode or corrosion resistance. The measurement was performed from 100 kHz to 10 mHz at room temperature with 0.5 cm^2 nickel plated as the working electrode; Ni as the opposite electrode; calomen electrode as the reference electrode.

The plating hardness was determined on the Duramin-UK hardness tester at the Department of Materials Technology/Military Technology Academy. The abrasion resistance of the coating was determined by ASTM-G77 measuring the abrasion resistance of materials using the TE97 (UK) Turning Method at the Institute of Mining Machinery - Thanh Xuan - Hanoi. Determination of adhesion of Ni - CeO_2 - CuO and Ni - cured composites was done by thermal shock method according to TCVN 4392: 1986.

The principleschema of determination of Ti-CBN plating's abrasive stability is shown in Fig. 3. According to,[23,24] the abrasion resistance is determined by grinding coefficient G in grinding process with speed of cylinderal grinding tool is: 24,000 r/min, the grinding depth is: F = 10 mm/min. G is calculated according to the formula (1):

$$G = \frac{V_W}{V_S} = \frac{Q_W}{Q_S} \quad (1)$$

In which: $V_W = a_e \times b_w \times L_w$ is volume of grinded metal, Q_W is volume of grinded metal per unit of grinding length, Q_S is volume of Ni-CBN coating per unit length and $V_S = \pi d_s \Delta r_s b$ is volume of grinding Ni-CBN coating with Δr_s the radius of the grinding tool, b is the length of grinding and d is the average value of the grinding tool before and after grinding.

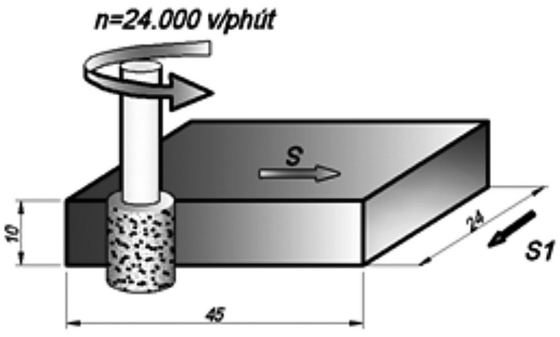

a)

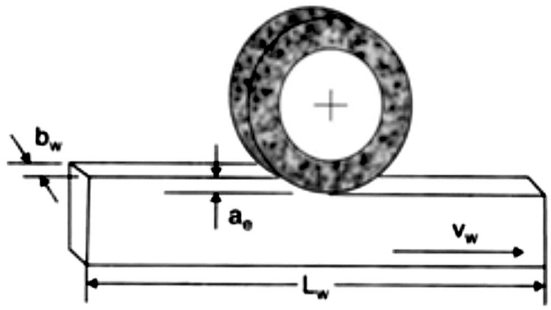

b)

Figure 3. The principal schema for evaluation of abrasion quality of the abrasive tools

3. RESULTS AND DISCUSSION

3.1. Catalytic function

3.1.1. Composition and structure of the plating

The content of nanoparticles CeO_2, CuO, ratio CuO/CeO_2 and total amount of CeO_2 and *CuO* on nanocomposite coatings obtained at the current density of 2 A/dm^2, temperature 50^{o}C, pH = 6 in solution of $NiSO_4$300 g/L, H_3BO_3 30 g/L, laurylsunphate 0.1 g/L, varified composition of CeO_2 and CuO in the solution with unchanged total of 8 g/L is presented in the table 1. The results of table 1 show that the composition of nanoparticles obtained on the coating depends on their composition in the plating solution. It is intent to increase while the amount of particles in solution rising to the highest value of 7 g/L. At this condition, the particle content on the coating increases to 37.22% for CuO and 34.68% for CeO_2, respectively. With the ratio of CuO/CeO_2 = 1, the content of CuO in the coating is 21.22%, higher than that of the CeO_2- 17.24%. In order toget higher content of CeO_2 on the coating, the ratio of CuO/CeO_2 = 3/5 should be used. This is may be because of the specific gravity of CuO, 6.31 g/cm^3, is smaller than that of CeO_2, 7.65 g/cm^3. The experimental results also show that the total content of CeO_2 + CuO on the coatings reaches the maximum value when the total one in the solution is 8 g/L. It is always less than 38.46%, while the total amount of particles in the solution is smaller or larger than 8 g/L. Thus, the content of the nanoparticles on the coating could becontrolled by varyingtheir composition in electrolyte solutions. Beside that, the galvanic parameters such as current density, time and speed of stirring solution also affect the amount of the nanoparticles on the nanocomposite layer. The results show that the total content of codeposition particles changes little around 36% while the plating time rising from 5 to 40 minutes, but reaches the highest value with current density of 2 A/dm^2 stirring speed of 600 r/min.

Table 1. Content of CeO_2 and CuO on the Ni-plating when changing of their content in the solution

C_{CeO_2} in electrolyte (g/L)	C_{CuO} in electrolyte (g/L)	C_{CeO_2} on the Ni-plating (%)	C_{CuO} on the Ni-plating (%)	Rate C_{CuO}/C_{CeO_2} on the plating	Total $C_{CeO_2} + C_{CuO}$ on the plating
1.0	7.0	2.25	37.22	16.54	39.47
2.0	6.0	4.12	34.64	8.41	38.76
3.0	5.0	5.04	31.08	1.23	36.12
4.0	4.0	17.24	21.22	1.23	38.46
5.0	3.0	20.13	17.36	0.86	37.49
6.0	2.0	31.46	6.28	0.20	37.74
6.4	1.6	31.90	4.46	0.14	38.18
7.0	1.0	33.78	3.46	0.10	37.24
7.2	0.8	34.68	2.15	0.06	36.83

Table 2 represents the total content of CeO_2 and CuO on the coatings obtainted under different conditions of pulse plating: average current densities i_{tb} = (2, 4, 6) A/dm^2; β = 0.2; α = 0.2; f = 100 Hz, the total content of particles of CeO_2 and CuO in the solution increases to 10 g/L. The results show that, the content of CeO_2 + CuO in the coating achieved to 28.46% when average pulse current density is 2 A/dm^2. This value is lower than that achieved by direct current becausein the pulse-current plating process, at the same current density, there is a dissolution of Ni on the cathode surface at half cycle, so the particles are not buried deeply in the plating layer and then easy to fall off the surface of the plating due to the collisions with

other particles from the motion caused by the stirring of the solution. When it increases up to 4 A/dm^2, the content of CeO_2 and CuO in the plating layer increases up to the maximum value of 37.69%. This phenomenon can be explained that at high enough current density, the amount of Ni formed on the electrode is large, as well as the amount of H_2 produced in the cathode due to the reduction of H^+ ions in the discharge solution is small, the CeO_2 and CuO solid particles are buried and stick well to the electrode, resulting in high amount of nanoparticles codeposited. At higher current density, i_{tb} = 6 A/dm^2, the content of particles on the coating decreases. This is because at higher average current density (cathode current density 7.5 A/dm^2), the nickel releasedmuch while the particle attached less, the H_2 gas formed by H^+ increases much more pushing the nano particles out of the electrode surface before they are buried by metal plating.

Furthermore, as the current density increases, the dischage rate of Ni^{2+} increases, but the speed of deposition of CeO_2 and CuO into the coating layer does not increase due to the diffusion of CeO_2 and CuO from the solution to the cathode surface is limited. This is similar to the process under direct current, so that the particle content on the coating reduces.

Table 2. Content of CeO_2 and CuO (% mass) on Ni-CeO_2-CuO nano composite plating with different pulse modes

Parameter	Pulse current density (A/dm^2)		
	i_c	i_a	i_{tb}
$\alpha = \beta = 0.2$	2.5	0.5	2.0
Particles content	28.46		
$\alpha = \beta = 0.2$	5,0	1,0	4,0
Particles content	37.69		
$\alpha = \beta = 0.2$	7,5	1,5	6,0
Particles content	32.18		

In order to create a plating, β- the ratio between anode current density and cathode current density inpulse current plating technology - could be changed but must be less than 1.

Table 3. Composition of CeO_2 and CuO particles on plating at different β values

B	α	i_c (A/dm^2)	i_a (A/dm^2)	i_{tb} (A/dm^2)	Particles content in plating (%)
0.1	0.2	4.9	0.49	4	34.51
0.2	0.2	5.0	1.00	4	37.69
0.3	0.2	5.1	1.53	4	28.62
0.4	0.2	5.2	2.08	4	13.04

The results of composition of platings fabricated in the sulphate solution under pulse conditions: average current density i_{tb} = 4 A/dm^2; α = 0.2; f = 100 Hz, plating time 20 minutes, CeO_2 25 g/L, CuO 5 g/L, stirring speed 600 r/min, β varying from 0.1 to 0.4 are shown in Table 3. From these results, it is found that, when increasing the value of β, the cathodic current of forming of nickel layer (i_c) does not change much while the anodic current of dissolving metal (i_a) increases. At a small value of β (0.1 ÷ 0.2), the increasing of β increases the relative speed of nickel formation, thus facilitating the adhesion of nanoparticles on the coating layer so the particle content on the plating layer increases. By continuously increasing of β value, the rate of nickel formation decreases leading to the falling of nano particles off the surface of the Ni coating due to insufficient nickel layer for burying nano particles. That will not be favorable for the deposition of the particles into the coating and the nano particle content in the coating layer also decreases. Burying particles into plating layer will be more difficult if increases β even further (β = 0.4). At $\beta \geq 0.3$, nanoparticles buried are poor, so obtained plating is smooth. Appropriate value of β is 0.1 ÷ 0.2, but the layer with the highest content of CeO_2 and CuO (37.69%) is created at β = 0.2.

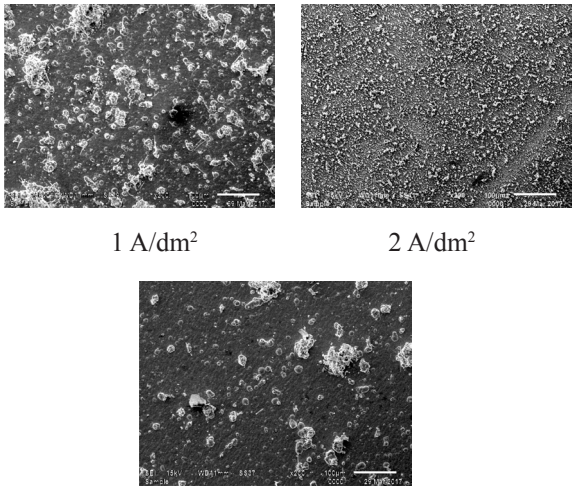

1 A/dm^2 2 A/dm^2

2 A/dm^2

Figure 4. The SEM images of the Ni-CeO_2-CuO surface plated at different direct current densities

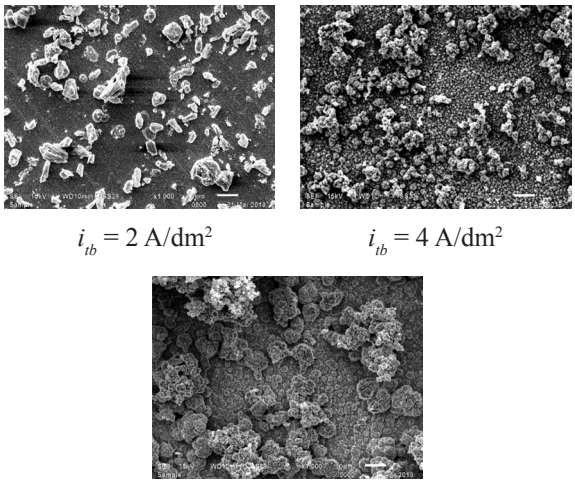

i_{tb} = 2 A/dm^2 i_{tb} = 4 A/dm^2

i_{tb} = 6 A/dm^2

Figure 5. The SEM images of the Ni-CeO_2-CuO surface plated with different pulsed current densities (i_{tb})

The surface morphology of Ni-CeO_2-CuO nano composite platings obtained from direct current electroplating as well as the pulse currentis evaluated using SEM images and presented in Figure 4 and 5. These images show that both the surface of the Ni-CeO_2-CuO coatings obtained by direct and pulse current have particles on surface that create porous structure, that increases when the current density as well as the concentration of nano particles on the surface get higher.

3.1.2. Corrosion resistance and abrasion resistance of the catalytic functional coating

The corrosion resistance of the Ni-CeO_2-CuO nano composite platingwas determined by the Tafel polarization measurement (Figure 6). From the Tafel curves shown in Fig. 6, it can be seen that the presence of CeO_2 and CuO inert particles makes negligible changes in the shape of polarization curves. That means the corrosion behavior of the nano composite platings similar to that of Ni plating in the experiment.

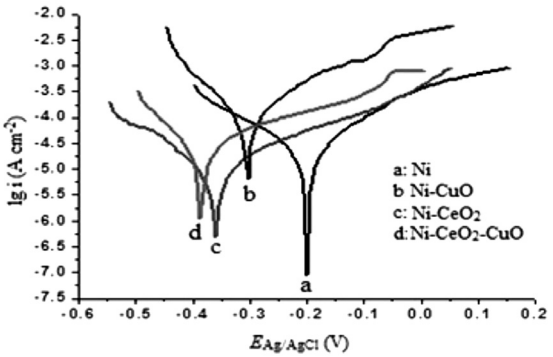

Figure 6. Tafel curves of the compositeplatings measured in NaCl 3.5%

However, from the tafel graph (Fig. 6), it is also found that the presence of CeO_2 and CuO particles on the nanocomposite plating of Ni-CeO_2-CuO changesthe values of corrosion potential (E_{Corr}), polarization resistance (R_P), and corrosion curent density (i_{Corr}) as well as corrosion speed (v_{Corr}) of the plating layer (Table 4). The results in table 4 show that the CeO_2 particles increase the polarization resistance on the nickel plating, reducing the corrosion current, while the CuO particles reduce the polarization resistance and increase the corrosion current. The Ni-CeO_2 nano composite plating has a lower corrosion current while Ni-CuO coating has a higher corrosion current than nickel one. The Ni-CeO_2-CuO nanocomposite plating has very small corrosion current that is approximately equal to the corrosion current as well as the corrosion rate of the nickel plating.

Table 4. Corrosion potential ($E_{Corr.}$), corrosion current density ($i_{Corr.}$), corrosion rate ($v_{Corr.}$), polarization resistance (R_p) of plating of Ni, Ni-CuO, Ni-CeO_2 and Ni-CeO_2-CuO

Plating layer	$i_{Corr.}$ (A/cm^2)	$E_{Corr.}$ (V)	R_P (Ω)	$v_{Corr.}$ (mm/year)
Ni	$1.688.10^{-5}$	- 0.198	$4.607.10^{2}$	0.2079
Ni-CuO	$8.871.10^{-5}$	- 0.303	$7.016.10^{1}$	1.0930
Ni-CeO_2	$0.809.10^{-5}$	- 0.363	$12.45.10^{2}$	0.0997
Ni-CeO_2-CuO	$1.601.10^{-5}$	- 0.339	$6.161.10^{2}$	0.1972

The results of the durability test in moist-heat accordance with TCVN 7699-2-30: 2007 as well as the durability in the saline moisture environment in accordance with TCVN 7699-2-52: 2007 with the 3rd level of extreme degree gave the comparable results between niken and Ni-CeO_2-CuO platings. These coatings neither peel off nor show rust, stains and abnormalities. Similarly, the results for adhesion of the Ni and Ce-NiO_2-CuO coatings according to TCVN 4392: 1986 with a heat shock of 300°C for 15 minutes show no evidence of peeling on the surface of two coatings, that demonstrates a good adhesion to ensure corrosion protection of the materials.

The abrasion resistance of the coating is evaluated through hardness and abrasion resistance. The average microhardness of 5 measurements for nickel plating is 163.16 HV, whereas it is 240.40 HV for the Ni-CeO_2-CuO coating, which is nearly 1,5 times higher than that of nickel. This may be due to the nature of the CeO_2, CuO particles as well as the particle size and surface structure of the plating layer which makes the surface hardness and thus increases the abrasion resistance. The average abrasion resistance is 19.35 g/Nm and 4.60 g/Nm for Ni and Ni-CeO_2-CuO platings, respectivesly, under measurement condition: 20 N load, rotation speed of 10 r/min, the circle diameter of 34.10^{-3}, and 169 seconds. Thus, the abrasion intensity of the Ni plating is 4.2 times (19.35/4.60) of the Ni-CeO_2-CuO composite coating. This means that the abrasion resistance of the Ni-CeO_2-CuO composite coating is 4.2 times greater than that of pure Ni plating. Similarly, the abrasive coeficient of Ni coating is 1.318 which is higher than that of the Ni-CeO_2-CuO nano composite plating of 0.274, which also demonstrates that the Ni-CeO_2-CuO composite coating is 4.2 timesmore durable than the Ni coating.

Thus, the corrosion and abrasive resistance of the Ni-CeO_2-CuO nano composite plating ensure the catalytic functionality of the coating is well utilized in the corrosive and abrasive environment of the catalytic box for engine exhaust gastreatment.

3.2. Self-cleaning superhydrophobic functional plating

3.2.1. Composition and structure of the plating

The discharge of nickel ion to form Ni-TiO_2 plating in electrolyte with different TiO_2 content is shown in Figure 7.

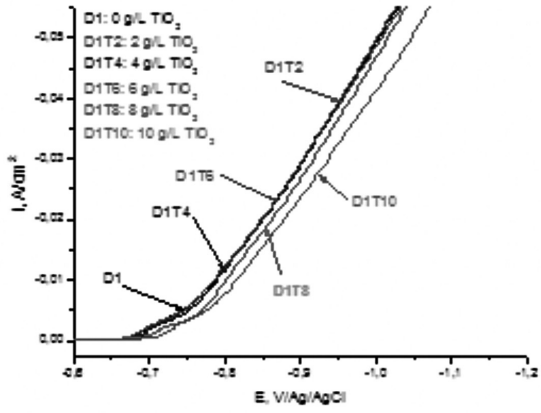

Figure 7. Cathodic polarization curve of Ni^{2+} discharge in electrolyte containing TiO_2 0 ÷ 10 g/L, 55°C, stirring solution, potential scanning speed 5 mV/s

Figure 7 shows that the cathodic polarization of the nickel-forming process is almost unchanged when TiO_2 is added in solution with a concentration of 2 ÷ 6 g/L, but it slighty increases if the TiO_2 concentration in the solution rising from 6 to 10 g/L. This is due to the fact that when the concentration of TiO_2 in the bath increases, the presence of

TiO_2 nanoparticles in the double layer increases reducing Ni^{2+} concentration on the cathode and therefore reducing the discharge rate as well as the rate of the nickel ions deposition, so that the cathode polarization increases. However, TiO_2 is electrochemical inert particle so that it has negligible effect on Ni^{2+} discharge.

XRD results todetermine the content of TiO_2 on Ni-TiO_2 coating formed at different plating time and direct current densities as well as different average pulse currentdensitiesare shown in Table 5 and Table 6, respectively.

Table 5. TiO_2 content on Ni-TiO_2 coatings obtained at different times and direct current densities

Plating time, min	Content of TiO_2, %			
	2 A/dm^2	3 A/dm^2	4 A/dm^2	5 A/dm^2
10	8.53	9.28	6.00	4.07
20	8.03	10.53	5.94	4.05
30	8.35	10.22	6.43	4.38

The results from Table 5 show that while the plating time of 10 to 30 minutes results in negligible change in the TiO_2 content on the composite coating, the curent density has strongly influences on it. In the curent density range from 2 A/dm^2 to 3 A/dm^2, the TiO_2 content increases and reaches the maximum value, but as the current density increases continuously, the TiO_2 content in the coating decreases sharply. It may be because of the large amount of H_2 formed at high current densities limiting co-precipitation of TiO_2.

Table 6. TiO_2 content on Ni-TiO_2 platings obtained at different pulse parameters

Parameter α, β	Masse of TiO_2 in plating, %		
	3 A/dm^2	5 A/dm^2	7 A/dm^2
$\alpha = \beta = 0.1$	0.22	0.78	1.05
$\alpha = \beta = 0.2$	1.78	0.48	2.55
$\alpha = 0.1$; $\beta = 0.2$	5.37	9.52	7.48
$\alpha = 0.2$; $\beta = 0.1$	12.30	10.47	8.67

The results in Table 6 show that the coatings obtaintedunder reversed squarepulse plating condition: frequency f = 100 Hz, average current density i_{tb}: (3, 5, 7) A/dm^2, $\alpha = \beta = 0.1$ and $\alpha = \beta = 0.2$ are thin, black, irregular with very small TiO_2 content ($\leq$ 2.55%). When $\beta = 0.2 > \alpha = 0.1$, with the increase of i_{tb} from 3 A/dm^2 to 5 A/dm^2, the TiO_2 content on the coating increases and then decreases as i_{tb} increases to 7 A/dm^2. This phenomenon can be explained as the increase of H_2 gas by the increase of current density decreases the amount of TiO_2coprecipitated with nickel, like under the direct current plating. Furthermore, as the current density increases, the rate of Ni^{2+} reduction increases, but the rate of deposition of TiO_2 particles into the coating does not increase due to the limited diffusion of TiO_2 from the solution to the cathode surface. As a result, the particle content in the coating decreases. When $\beta = 0.1 < \alpha = 0.2$, with the increase of i_{tb} from 3 A/dm^2 to 7 A/dm^2, the TiO_2 content on the plating layer decreases. Under this condition, the coating is light and equally. At the same average current density of 3 A/dm^2, the TiO_2 content on the plating formed under pulse currentis higher than that of direct one, the corresponding values are 12.30% (Table 6) and 10.53% (Table 5). This is also due to the fact thatthe pulse current used is reversed one so that at the half cycle in which anode becomes cathode, there is no H_2 released, therefore, the H_2 released is less than in direct current case and then the push nano inert particles off the electrode surface of hydrgen gas reduces. The high ability to adhere on the surface of the inert particles increases the possibility of particles buried into the plating layer, so their content on the plating layer is high.

SEM images of surface of Ni and Ni-TiO_2 composite coatings fabricated at curent density of 3 A/dm^2 in 20 minutes are shown in Figure 8. The Ni-TiO_2 nano composite plating formed at this condition has 10.53% (by weight) TiO_2 in the plating layer, surface morphology is uneven but the roughness is greater than that of the pure Ni.

Therefore, the hydrophobicity is higher (contact angles are 164.7° and 125.7° respectively). The surface energyis 6.623 mN/m for the Ni plating but only is 0.055 mN/m for the Ni-TiO_2 plating.

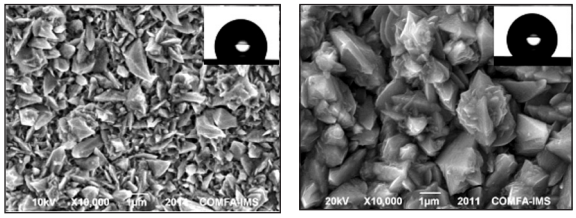

Figure 8. SEM images of Ni plating (a) and Ni-TiO_2 nanocomposite plating (b) formed at 3 A/dm^2 in 20 minutes with the same magnification of 10,000

The nanocomposite plating generally has finer crystalline structure than pure metallic coating[25]. However, as the amount of nanoparticles in the electrolyte increases to a certain value, it increases the roughness of the coating[2]. The pure nickel plating formed in $NiCl_2$ solution is not a fine-grained one with uneven surface texture, but it's roughness is not too high so it is only a hydrophobic surface with the water contact angle is low of 125.7°, meanwhile the Ni-TiO_2 composite coating has higher roughness with heriachial structure which leads to super hydrophobicity with contact angle of 164.7°.

The Ni-TiO_2 platings formed under pulse current have less rough surface structure than ones formed under direct one and their surface morphology change when α increased from 0.1 to 0.2 (Fig. 9). With this increase of α, the content of TO_2 on the plating increases and thus increases the roughness as well as the hydrophobicity of the coating. When α increases to 0.3, the TiO_2 content on the plating reduces slightly, the surface morphology of the coating is different from that of α = 0.2.

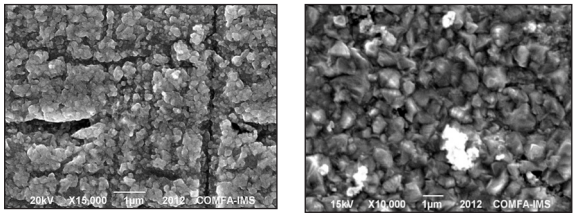

a) 112,21° b) 136,68°

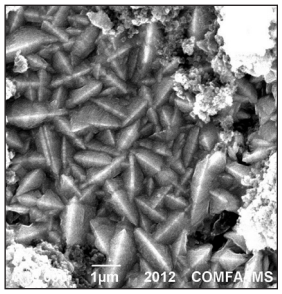

c) 135,00°

Figure 9. SEM images and contact angle values of Ni-TiO_2 nanocomposite coating formed under different values of α: a) α = 0.1; b) α = 0.2; c) α = 0.3

However, all these coatings have rough surface and are the hydrophobic surfaces with contact angle ≈140°, water droplets can easily roll off the surface when the surface are tilted a very small angle.

3.2.2. Corrosion resistance of hydrophobic plating

The corrosion resistance of the nickel-plated layers was investigated by measuring corrosion current and electrochemical impedance. Fig. 10 and Table 7 are the results of the corrosion current measurement of nickel plating and Ni-TiO_2 nanocomposite platings in 3.5% NaCl solution.

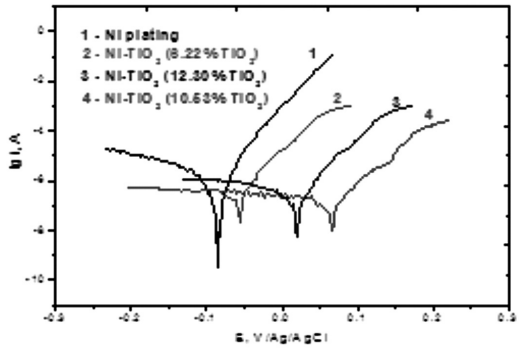

Figure 10. Tafel curves of Ni plating and Ni-TiO_2 nanocomposite platings in 3.5% NaCl solution

Table 7. Corrosion current measurements of platings of nickel in a 3.5% NaCl solution

Plating	% TiO_2	Contact angle, degrees	$E_{Corr.}$ (V)	$i_{Corr.}$ (A/cm^2)	$v_{Corr.}$ (mm/year)
Ni	0	125.70	-0.089	$2.10.10^{-6}$	$6.71.10^{-3}$
Ni-TiO_2	6.22	152.80	-0.054	$3.41.10^{-7}$	$1.09.10^{-3}$
Ni-TiO_2	10.53	164.66	0.067	$2.23.10^{-7}$	$1.13.10^{-4}$
Ni-TiO_2	12.30	136.68	0.020	$6.52.10^{-7}$	$2.08.10^{-3}$

The results of Fig.10 show that the Tafel curves of the Ni and Ni-TiO_2 coatings are similar, but the corrosion potentialsof the Ni-TiO_2 coatings strongly change to the positive side, which means that the cathodic process is inhibited. As the results presented in Table 8 show that the corrosion currents of the Ni-TiO_2 coatings are smaller than those of Ni. This is consistent with published studies[9,26,27] suggesting that the highly corrosion-resistant TiO_2 nanoparticles involve in the coating would act as a barrier to reduce the surface area of the coating exposing to the corrosive environment leading to reduced corrosion rate. In addition, TiO_2 nanoparticles alter the nickel-plated surface morphology which increases hydrophobicity of the coating, thereby reducing moisture retention, reducing the ability of forming the electrolyte environment on the surface of the coating which decrease the ability of being corroded of the coating.

The durability of the Ni and Ti-TiO_2 coatings in the chemical environment was investigated with solutions of NaCl 3.5% and HCl 1 M. The Ni-plating is chemically stable in alkaline environment due to formation of nickel hydroxide film which is durable to the corosion but it will be corroded in saline and is unstable in acidic environment as well as slowly dissolved in dilute acid solutions[19]. Table 8 shows the results of determination of corrosion speed of Ni and Ni-TiO_2 coatings in NaCl and HCl environments.

Table 8. Mass reduction (mg/cm^2) of Ni and Ni-TiO_2 platings after immersion in NaCl and HCl solutions

Platings	NaCl solution			HCl solution		
t, h	24	48	72	24	48	72
Ni	0.33	0.90	0.93	3.23	5.47	6.23
Ni-TiO_2	0.07	0.10	0.12	0.97	2.63	3.67

The results show that the nickel plating is stable in saline, slowly corroded in acidic environment. The reduced mass of Ni-TiO_2 coatings in the NaCl and HCl environment is much smaller than that of Ni-plating. This is due to the hydrophobicity of the Ni-TiO_2 coatings obtained from the chloride solution.

The results of microhardness of the nickel plating and Ni-TiO_2 platings are shown in Table 9. The hardness of electroplating depends on some factors as following: structure and mechanical properties of plating metal; coating surface mophology; conten of particles on coating; the shape and size of codeposited particles. In this case, the structure and mechanical properties of the metal matrix, particle size and shape are almost unchanged with different content of nano particles on the coatings, so the hardness of these coatings depends largely on the morphology of the coating surface and the particle content on the coating. The Ni-TiO_2 coating formed under pulse current has less rough surface and higher particle content on the coating so that it has higher hardness than plating formed by direct current. The Ni-TiO_2 nano composite platings formed from direct current have similar surface morphology, so the hardness increases with the particle content on the plating and is higher than that of the pure metal.

Table 9. Results of microstructure hardness testing (HV 0.01) of nickel plating

Plating layer	1	2	3	4	5	Average
Ni	250.7	253.7	250.7	250.7	253.7	251.9
Ni-TiO_2	343.3	338.6	334.1	343.3	338.6	339.6

The results show that the abrasion and corrosion resistance of Ni-TiO_2 composite are better than that of Ni.

3.3. Ni-CBN microcomposite functional plating for grinding, cutting

3.3.1. The distribution and bury of particles on Ni-CBN microcomposite plating

The functional plating that used as grinding, cutting tool must have reasonable density of the abrasive particles on the surface, and the particles need to be buried enough in the plating layer to have strong bond with the surface Controlling the influence of technical factors such as current density i, A/dm^2; the rotation speed of cathode n, r/min and the plating time t, min may create Ni-CBN platings with a good distribution and optimal buried for the practical application. The actual particle distribution K_{PBT} is counted from the software from the SEM image of the Ni-CBN plating surface with reasonable magnification (Figure 11). The dependence of K_{PBT} on the plating technology elements mentioned above can be described by the mathematical model elaborated from the practical planning (Table 10 and 11) as follows:

$$K_{PBT} = f(n, i, t) \quad (2)$$

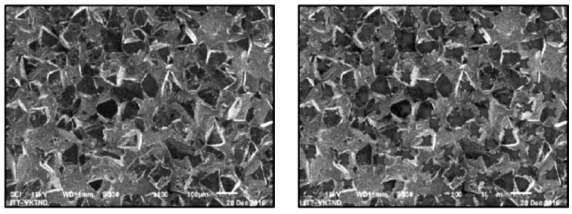

Figure 11. SEM images and results of counting the number of particles distributed on the surface of the Ni-CBN microcomposite plating

Sample: M14; Position: 2; Practicle number: 92; Area: 1.226 mm^2; Density: 75.04 praticle/mm^2.

Table 10. The real variable and encoded variables from three plating factors: mixspeed (n), time (t) and curent density (i).

Variables	The real variable			Encoded variables		
	n, r/min	t, min	i, A/dm^2	A	B	C
Above level (+1)	1.3	10	8	+1	+1	+1
Lower level (-1)	0.7	5	3	-1	-1	-1
Variable range	0.6	5	5			

The variability of the selected factors for the model (Table 11) is: i varies in range of (3 ÷ 8) A/dm^2 because of the large grinding grain (≈100 μm), then i must be large enough to create enough Ni to keep seeds on the surface; n is selected in range of (0.7 ÷ 1.3) rpm, because if n is large, the particles could not adhere and be kept on the surface of the sample; otherwise, if n is too small, the particles are distributed unevenly; the t is selected in range of (5 ÷ 10) minutes, when t is small, particle distribution is unevenly, while with large value of t, particles are overlapping on the sample surface. The results of K_{PBT} determination with the variables of plating parameters as shown in Table 10 are presented in Table 11.

Table 11. Experimental results of the effect of three factors: n, t and i

TT	Encoded variables			The real variable			K_{PBT}
	A	B	C	n, r/min	t, min	i, A/dm^2	
1	-1	-1	-1	0.7	5	3	76.26
2	+1	-1	-1	1.3	5	3	69.74
3	-1	+1	-1	0.7	10	3	84.01
4	+1	+1	-1	1.3	10	3	79.93
5	-1	-1	+1	0.7	5	8	91.35
6	+1	-1	+1	1.3	5	8	83.61
7	-1	+1	+1	0.7	10	8	99.10
8	+1	+1	+1	1.3	10	8	88.91
9	-1	0	0	0.7	7.5	5.5	83.61
10	+1	0	0	1.3	7.5	5.5	79.12
11	0	-1	0	1	5	5.5	77.08
12	0	+1	0	1	10	5.5	84.01
13	0	0	-1	1	7.5	3	76.26
14	0	0	+1	1	7.5	8	92.17

15	0	0	0	1	7.5	5.5	81.16
16	0	0	0	1	7.5	5.5	81.57
17	-1	-1	-1	0.7	5	3	75.04
18	+1	-1	-1	1.3	5	3	70.96
19	-1	+1	-1	0.7	10	3	83.20
20	+1	+1	-1	1.3	10	3	79.12
21	-1	-1	+1	0.7	5	8	89.72
22	+1	-1	+1	1.3	5	8	81.57
23	-1	+1	+1	0.7	10	8	96.25
24	+1	+1	+1	1.3	10	8	87.28
25	-1	0	0	0.7	7.5	5.5	84.01
26	+1	0	0	1.3	7.5	5.5	78.71
27	0	-1	0	1	5	5.5	79.12
28	0	+1	0	1	10	5.5	86.46
29	0	0	-1	1	7.5	3	79.12
30	0	0	+1	1	7.5	8	90.54
31	0	0	0	1	7.5	5.5	83.61
32	0	0	0	1	7.5	5.5	79.12

$$K_{PBT} = 70.42 - 3.13n + 1.476t - 0.049i + 0.3586i^2 - 1.359n \times i \quad (3)$$

From the regression equation 3, we have examined the standards and found the tendency and the influence of factors of the plating technology. The rotation speed of cathode n has the coefficient -3.13 which means that the K_{PBT} will decrease as n increases. Coefficient of plating time is 1.476 which shows that K_{PBT} increases when plating time increases. The coefficients of current density i and i^2 are -0.049 and 0.3586, respectively, thus the effect of $i$on K_{PBT} is non-linear. The interaction of these two factors, $n \times i$, also reduces the K_{PBT} coefficient due to the negative coefficient.

3.3.2. Corrosion and abrasion resistance of Ni-CBN microcomposite coatings

The abrasive and grinding functional plating, which based on the codeposition of CBN grinding particles with metal nickel plating, need to be determined the corrosion resistance to ensure the stability of the grinding material as well as the tool made from these platings. Cutting grinding is made from this functional plating. Figure 12 shows the Tafel curves of nickel and Ni-CBN microcomposite coatings made under different current densities.

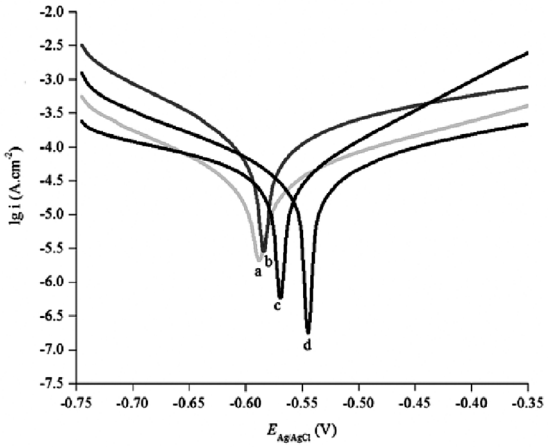

Figure 12. Tafel curves of nickel plating (b) and Ni-CBN microcomposite coatings (a, c, d) made under with different current densities: a) 1.5 A/dm^2; c) 2.0 A/dm^2 and d) 2.9 A/dm^{2}in NaCl 3,5%. The plating condition is: CBN concentration 30 g/L; plating time for L_1 (Liner layer), L_2 (CBN mount layer) and L_3 (buried layer) corresponding to (5/5/15) minutes; temperature of electrolyte is 55^{o}C.

From Figure 12, it can be seen that the presence of inert CBN particles increasesthecathodic and anodic polarization as well as shifts the corrosion potential to the positive side, in which the coating obtained at a plating current density of 2.0 A/dm^2 has the highest effect. Table 12 presents the values of corrosion potential, corrosion current, and corrosion rate of Ni-CBN layers produced at different plating current densities.

Table 12. Corrosion characteristic obtained from potentiodynamic polarization measurement for pure Ni coating and Ni-CBN microcomposite coatings plated at different current densities in 3.5% NaCl solution

Sample		i, A/dm^2	$i_{Corr.}$, A/cm^2	$E_{Corr.}$, V	R_P, Ω	$v_{Corr.}$, mm/year
b	Ni	0	$1.915.10^{-5}$	-0.584	$3.386.10^{1}$	$1.056.10^{-1}$
a	Ni-CBN	1.5	$8.426.10^{-6}$	-0.589	$1.500.10^{2}$	$4.646.10^{-2}$
d	Ni-CBN	2.0	$7.713.10^{-6}$	-0.545	$1.146.10^{2}$	$4.253.10^{-2}$
c	Ni-CBN	2.9	$9.478.10^{-6}$	-0.570	$1.093.10^{2}$	$5.227.10^{-2}$

The results from Table 12 also show that the corrosion current densities of Ni-CBN platings reduce to nearly half the Ni plating while the corrosion potentials reduce slightly, but the polarization resistances decrease dramatically. This indicates that the presence of inert CBN particles reduces the surface area of the nickel metal layer, thus reduces the corrosion rate of the nickel metal.

The durability of the bonding between CBN with Ni layer that were formed by the nickel plating process from the Watts solution containing CBN particles needs to be evaluated to determine the ability to retain the grinding grain during grinding or cutting. If the bonding between CBN grinding particles and Ni-plated metal, between the Ni-plated metal and the surface of the steely core of grindstoneis not sufficiently durable, the grinding particles will be separated from the binder, the surface of grindstone will be seperated from the suface of the core. As there have been no method to assess the durability of the bonding bridges, the bond strength test between the grinding particles and the binder is carried out by the experimental grinding process to obtain a general view of the quality of the link created by the plating process. The durability of the produced bonding bridges as well as the cutting properties of produced grindstone can be evaluated by observing the grindstone surface after grinding on the scanning electron microscope, measuring the surface roughness and the extracted metal volume. Table 13 presents the relationship between time, current density of plating layers: Ni (L_1), Ni with mounted CBN (L_2) and Ni to bury CBN (L_3) with distribution coefficient of CBN particles (K_{PBT}) on the surface of grinding functional microcomposite plating formed at 55°C, rotation speed of cathode 0.7 rpm/min.

Table 13. The distribution coefficients of CBN particles on the surface of platingsobtained at different current densities and plating times

Sample	Plating layer	*t*, minute	*i*, A/dm^2	K_{PBT}, particles/mm^2
M_1	L_1	25	3	84.01
	L_2	10	3	
	L_3	35	3	
M_2	L_1	25	3	99.10
	L_2	10	8	
	L_3	30	3	
M_3	L_1	25	3	76.26
	L_2	5	3	
	L_3	35	3	
M_4	L_1	25	3	91.35
	L_2	5	8	
	L_3	30	3	

As can be seen in Table 13, the number of CBN particles on the coating surface is high value of 91.35 to 99.1 particles/mm^2 when the current densities of L_2 is higher than the current densities of L_1 and L_3, or plating time for burying layer is only 30 minutes.

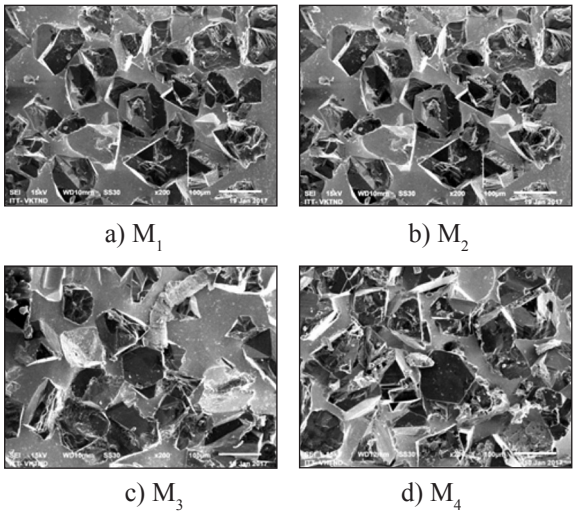

a) M_1 b) M_2

c) M_3 d) M_4

Figure 13. SEM image of abrasive surface after 200 grinding process

Figure 13 shows the SEM images of the samples of Table 13 after 200 abrasion cycles (equivalent to the abrasive time of 30 minutes). The steel material SKD 11 for cutting have been heat treated and have a hardness of 63 HRC. The

deep of cutting is 0.01 mm. The SEM images show no evidence of abrasion of the abrasive particles on the grindstone surface. Grinding particles involving in cutting and grinding metal without being turned off from the surface of grinding tool exhibiting that the nickel bonding bridge formed by electroplating is sufficiently stable to keep the CBN particles out of abrasion under grinding force while CBN particles joining in cutting or abrasiving process of metals. This is the insurance of the stability of bonding bridge. It can be concluded that the depth of 55% CBN buried in the nickel plating has created a good bond between the grinding particles and the plating metal and the holding force is strong enough to with stand the impact of grinding force in cutting process without separating from the surface of abrasiving tool.

4. CONCLUSION

Functional electroplatings have been fabricated by combining nickel plating formed from $NiSO_4$, $NiCl_2$ or Watts solutions with nanoscale or micron particles, in which Ni-CeO_2-CuO plating has catalytic function, Ni-TiO_2 plating is hydrophobic and sefl-cleaning material, Ni-CBN plating can be use as cutting and grinding tool.

The content of the functional particles, the proportion and distribution of the particles in the platings as well as the degree of adhesion, cohesion and depth of buried particles in the platingscan be controled by controlling the parameters of the plating technique such as the concentration of inert particles in the plating solution, current density, or curent characteristics, polarization potential, plating time and stiring speed.

EDX results and SEM images have demonstrated the presence on the Ni plating of CeO_2-CuO nanoparticlesmixture, 36.12% to 39.87% wt, and TiO_2 particles, upto 10.53% wt, CBN, 69.74 particles/mm^2 to 99.10 particles/mm^2, with corresponding revelation on the surface platings. The determination of the catalytic activity, hydrophobicity and cutting abrasion have demonstrated the catalytic, hydrophobic, and abrasive cutting functions of Ni-CeO_2-CuO, Ni-TiO_2 and Ni-CBN, respectively.

Corrosion resistance and hardness of all functional coatings are higher than that of pure nickel plating. Specifically, the corrosion rate of Ni-CeO_2-CuO coating is 1.601×10^{-5} A/dm^2 (0.1972 mm/year), of Ni-TiO_2 coating is 2.23×10^{-7} A/dm^2 (1.14×10^{-4} mm/year and of Ni-CBN platingis $7{,}713\times10^{-6}$ A/dm^2 (4.253×10^{-2} mm/year). The abrasion resistance of the Ni-CeO_2-CuO coating is 240.4 HV, 1.5 times higher than Ni plating, and that of the Ni-CBN coating is 63 HRC of the heat treated steels SKD 11. These results confirm that the funtional platings are stable enough to the environment and can work stably for efficiency.

REFERENCES

1. Guglielmi N. Kinetics of Deposition of Inert Particles from Electrolytic Baths, *Journal of Electrochemical Society*, **1972,** *119 (8)*, 1009-1012.

2. Ngô Thị Ánh Tuyết, Nguyễn Ngọc Phong, Nguyễn Viết Huệ. *Nghiên cứu ảnh hưởng của các hạt trơ đến tính chất của lớp mạ composit niken,* Tuyển tập các công trình khoa học Hội nghị toàn quốc Điện hóa và Ứng dụng lần thứ 2, **2006**, 121-125.

3. C.T.J.Low, Wills R.G.A., Walsh F.C. Electrodeposition of composite coatings containing nanoparticles in a metal deposit, *Surface & Coatings Technology*, **2006,** *201,* 371-383.

4. L. Timoshkov, V. Kurmashev, and V. Timoshkov. Electroplated Nanocomposites of High Wear Resistance for Advanced Systems Application, *Advances in Nanoccomposites Technology*, *Dr A. Hashim (Ed.), InTech*, **2011**, pp. 953-78.

5. Phong Nguyen Ngoc, Hue Nguyen Viet, San Pham Thy, Tuyet Ngo Thi Anh. *Electrochemical properties of Ni/nano composite plating*, *Journal of Science and Technology*, **2010**, *48 (5A)*, pp. 92-95.

6. Nguyen Duc Hung, Tran Thi Van Nga, Mai Van Phuoc. Thickness determination and control of function Ni-Composite electrodeposited coatings, *Journal of Science and Technology*, **2017,** 55 (B1), 1-6.

7. Nguyễn Đức Hùng, Phạm Xuân Điệp, Lã Ngọc Hùng, Lê Thị Phương Thảo, Đào Khánh Dư. Đặc tính của lớp mạ niken compozit nano xeri điôxit, *Tạp chí KH&CN,* **2013,** *Tập 51(3A)*, 219-229.

8. N. S. Qu, W. H. Qian, X. Y. Hu, and Z. W. Zhu. Fabrication of Ni-CeO_2 Nanocomposite Coatings Synthesised via a Modified Sediment Co-Deposition Process, *International Journal of Electrochemical Science*, **2013,** 8 (9), 11564-77.

9. Ranjan Sen, Siddhartha Das, Karabi Das. Effect of stirring rate on the microstructure and microhardness of Ni-CeO_2 nanocomposite coating and investigation of the corrosion property, *Surface & Coatings Technology*, **2011**, *205*, 3847-3855.

10. Mai Van Phuoc, Nguyen Duc Hung. Some factors affecting on the composition of CeO_2 and CuO in Ni-CeO_2-CuO composite plating coating, *Tạp chí Nghiên cứu Khoa học và Công nghệ quân sự*, **2018,** Số đặc san, 130-135.

11. S.A. Lajevardi, T. Shahrabi. Effects of pulse electrodeposition parameters on the properties of Ni-TiO_2 nanocomposite coatings, *Applied Surface Science*, **2010**, *256*, 6775-6781.

12. Huang Siya, Hu Yawei, Pan Wei. Relationship between the structure and hydrophobic performance of Ni-TiO_2 nanocomposite coatings by electrodeposition, *Surface & Coatings Technology*, **2011,** 205, 3872-3876.

13. Z Shi, S. Malkin. Wear of Electroplated CBN Grinding Wheels, *Transactions of the ASME*, **2006**, 128, 110-118.

14. Z. Shi và S. Malkin. An Investigation of Grinding with Electroplated CBN Wheels, *CIRP Annals - Manufacturing Technology*, **2003**, *52(1)*, 267-270.

15. Marius Winter, et al. Life cycle assessment of cubic boron nitride grinding wheels, *Journal of Cleaner Production*, **2015**, *107*, 707-721.

16. Hua-Yun You, et al. Design and application of CBN shape grinding wheel for gears, *International Journal of Machine Tools and Manufacture,* **2003,** *43(12)*, 1269-1277.

17. P. Baghery, M. Farzam, A. B. Mousavi, M. Hosseini. Ni-TiO_2 nanocomposite coating with high resistance to corrosion and wear, *Surface & Coatings Technology*, **2010**, *204*, 3804-3810.

18. Mai Van Phuoc, Nguyen Duc Hung. Corrosion protection and chacracteristics of Ni-CeO_2-CuO electroplating layer on steel substrate, *Journal of Science and Technology*, **2017,** *55 (5B)*, 181-186.

19. Maria Lekka, et al. Corrosion and wear resistant electrodeposited composite coatings, *Electrochimica Acta*, **2005,** *50(23)*, 4551-4556.

20. Ibl N. Some theoretical aspects of pulse electrolysis, *Surface Technology*, **1980,** *10*, 81-104.

21. N. V. Mandich. Pulse and pulse-reverse electroplating, *Metal Finishing*, **2002,** *100 (1)*, 359-364.

22. Denny Thiemig, Ronny Lange & Andreas Bund. Influence of pulse plating parameters on the electrocodeposition of matrix metal nanocomposites, *Electrochimica Acta*, **2007,** *52 (25)*, 7362-7371.

23. Trần Thị Vân Nga. *Nghiên cứu chế tạo đá mài CBN liên kết kim loại bằng phương pháp mạ điện và đánh giá tính cắt của đá mài*, luận án tiến sĩ, Viện Nghiên cứu Cơ khí, 2016.

24. Hans Kurt Toenshoff, Berend Denkena. *Basics of Cutting and Abrasive Processes*, 2013938164, ed, Springer, Springer Heidelberg New York Dordrecht London, 2013.

25. Low C.T.J., Wills R.G.A., Walsh F.C. Electrodeposition of compositecoatings containing nanoparticles in a metal deposit, *Surface & Coatings Technology,* **2006,** *201*, 371-383.

26. T. Darmanin, E. Taffin de Givenchy, S. Amigoni, F. Guittard. Superhydrophobic Surfaces by Electrochemical Processes, *Advanced Material,* **2013,** *25*, 1378-1394.

27. W. Shuai, L. Qingwen, Z. Yang, W. Shaodan, L. Yaoxian, Y. Qingbiao, S. Yan. Preparation of a multifunctional material with superhydrophobicity, superparamagnetism, mechanical stability and acids-bases resistance by electrospinning, *Applied Surface Science*, **2013**, *279*, 150-158.